RADIO OBSERVATIONS RELATED TO STAR FORMATION

P. G. Mezger and Lindsey F. Smith
Max-Planck-Institut für Radioastronomie
Bonn, FRG

I. AN OVERVIEW

1) Some Basic Facts

Stars form out of the interstellar gas. Their observed masses range from O.08 to $\sim$100 $M_\odot$. The birth rate of stars or the initial mass function (IMF) decreases rapidly with increasing stellar mass, approximately $\propto M^{-1.35}$ according to Salpeter (1955). There is no reason to believe that protostars with masses less than O.08 $M_\odot$ do not form and contract; however, they will never become main sequence (MS) stars. Stars with masses higher than 100 $M_\odot$ can exist as stable MS stars with lifetimes of $\sim$10^6 yr; however, radiation pressure acting on dust grains prevents their formation (Larson and Starrfield, 1971). For single protostars to contract, densities of 10^3 to 10^6 atoms cm^{-3} are required. The average density of the interstellar gas is about 1 atom cm^{-3}. Therefore, the formation of dense and cool clouds in the interstellar gas must be the first step in the evolutionary track of stars forming out of the interstellar matter. About 60% of the total mass of interstellar gas in our Galaxy is contained in clouds with total densities of some 10^2 cm^{-3} or more (Mezger and Smith, 1975); most of these clouds are located within galactic radii 4 to 13 Kpc and in the inner part of the gaseous nuclear disk which surrounds the nucleus of the Galaxy. These are also the regions in our Galaxy where, at present, most stars are being formed.

While the IMF in the solar vicinity increases steadily up to the lower limit of stellar masses, the IMF of open clusters turns over at about 1 $M_\odot$ (van den Bergh, 1961. See also Fig. 11 and Sect. III.2).*)

---

*)Herbig (priv. comm.) informs us that the stellar mass at which this turnover occurs, varies from cluster to cluster. For the sake of simplicity we continue to define low-mass stars by < 1 $M_\odot$ and cluster stars (or higher mass stars) by $\gtrsim 1$ $M_\odot$.

This suggests that the IMF in the solar vicinity is the result of a superposition of two rather independent mechanisms of star formation: All OB stars and most of the higher mass stars $\gtrsim 1$ $M_\odot$ are formed in open clusters and OB associations. Low mass stars < 1 $M_\odot$ on the other hand apparently can form as single stars out of relatively small and dense clouds (Herbig, 1970). We suggest that low-mass stars form rather continuously out of dense cloudlets or small condensations in extended tenuous molecular clouds; but that these two processes are not mutually exclusive: O stars may eventually form in extended clouds where, for a long time, only low-mass stars have formed. It has been suggested that T-Tauri associations represent the earlier stage and that they may eventually become OB associations (Mezger, 1971).

Where do stars form? In the following, we discriminate between main spiral arms and large cloud complexes in the interarm region. We also discriminate between giant HII regions, which require several early O stars, and small HII regions, which require only one O or B star, to account for their ionization. (Somewhat arbitrarily, the intrinsic flux density of a giant HII region is defined as $S_5 D^2 \geq 400$ (f.u.) (Kpc)^2, which is four times the intrinsic flux density of Orion A.) Giant HII regions are known to define the main spiral structure in external galaxies. Georgelin and Georgelin (1976) used this fact to determine the spiral structure of our Galaxy on the basis of optical and radio observations of giant HII regions. They can locate all observed giant HII regions in four main spiral arms between galactic radii 4 and 13 Kpc, each winding about 3/4 of a revolution around the galactic center (Fig. 1). Note, however, that some of the largest HII regions are located in the central part of the nuclear disk, < 200 pc from the nucleus of our Galaxy. A large number of small HII regions are located between the main spiral arms, and are often associated with dense clouds (CO-clouds). These small HII regions represent O star formation in the interarm region. By counting Lyman continuum (Lyc) photons, Mezger and Smith (1975) estimate the present birth rate of O stars and find that about 70% are formed in main spiral arms and the rest are formed (in about equal fractions) in cloud complexes in the interarm region and in the inner part of the nuclear disk.

Formation of star clusters in main spiral arms and in cloud complexes in the interarm region can probably account for the formation of all OB stars (Roberts, 1957) and hence of most of the higher-mass stars $\gtrsim 1$ $M_\odot$. Where do low-mass stars < 1 $M_\odot$ form? As will be shown in Sect. II, radio observations can not help to answer this question. But one can easily show that less than 1% of the interstellar matter contained in clouds within galactic radii 4 and 13 Kpc is transformed into cluster stars while passing through a main spiral arm (see, e.g. Mezger, 1975). The main effect of compression of interstellar gas entering spiral arms appears to be the production of clouds, of which only a small fraction collapses further and forms O star clusters and associations in the main spiral arm. Most of these clouds appear to travel as relatively stable objects into the interarm region and it may be within these clouds that low-mass stars form.
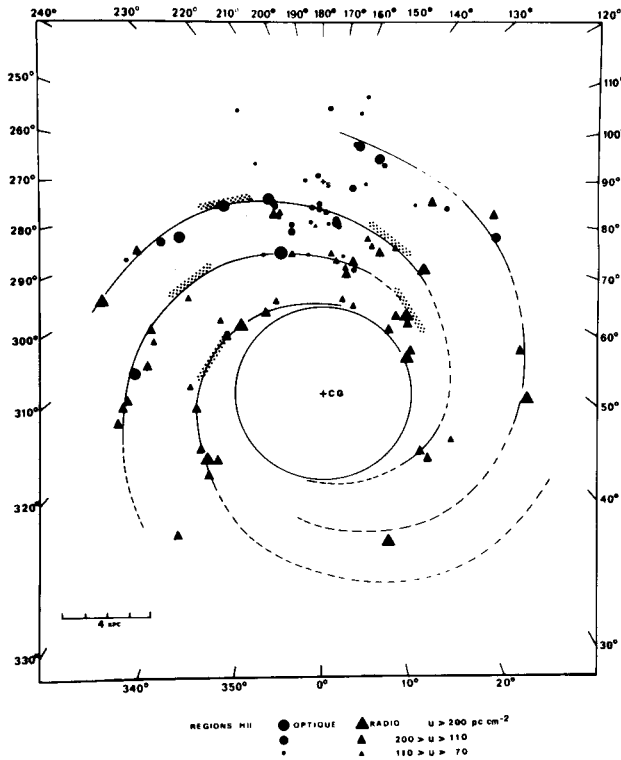
Figure 1: Main spiral
arms in the Galaxy,
determined from the
distribution of giant
HII regions by George-
lin and Georgelin (1976)

For stars $\gtrsim 1$ M$_\odot$, the units of star formation have been recognized as
clusters or sub-groups which contain some 1 000 M$_\odot$ of stars (Blaauw,
1964). There is no observational support for a picture where sub-groups
form as the result of a central collapse of a spherical cloud. It rather
appears that, in proto-clusters, physical conditions are such that single
stars can form and that stars of ~ 1 M$_\odot$ form first, followed by the for-
mation of higher mass stars and ending with the formation of O stars
(Iben and Talbot, 1966; Williams and Cremin, 1969).

What initiates star formation? As far as low-mass stars are con-
cerned, we know nothing. As far as OB stars are concerned, we know that
all giant HII regions, each of which contains several subgroups of O
stars, are located in one of the four main spiral arms or in the central
part of the nuclear disk; in cloud complexes in the interarm region ap-
parently only one OB cluster forms at a time although these clouds are
nearly as massive as those associated with giant HII regions. This sug-
gests that, in main spiral arms and in the central part of the nuclear
disk, large-scale effects, causing a sudden compression of the inter-
stellar gas, initiate collective star formation. In the interarm region,
star formation appears to be dominated by more local effects, whose na-
ture is not yet fully understood. Shock waves induced by supernovae may
be a possible mechanism. Observations related to the formation of indi-
vidual OB stars, clusters and associations will be reviewed in Sect. II.

Stars form out of the interstellar gas and, in their final stages, return part of their mass to the surrounding interstellar matter, enriching it with elements heavier than H. Therefore, the formation rate of massive stars is directly linked to the chemical composition of the interstellar gas. Today, in the solar vicinity, the mass fractions of elements are $X(^1H) = 0.70$, $Y(^4He) = 0.28$ and $Z(A>4) = 0.02$. In other regions where more or less gas has been transformed into stars and subsequently returned to the interstellar matter, one expects metal abundances to be different from those observed for the solar vicinity. The connection between star formation rate and gas-to-total mass ratio on the one hand and between star formation rate and chemical composition on the other hand is investigated in Sect. III.

2) Radio and Sub-mm Observations Related to Star Formation

Most stars form inside dense clouds where they can not be observed at optical wavelengths. Which kind of information related to the process of star formation can we hope to obtain from observations in the radio and sub-mm range? The main constituent of dense clouds is molecular H, which is unobservable in the radio range. However other molecules such as CO, CS, HCN, NH_3 and H_2CO, which have transitions in the radio range, also exist in rather large numbers. Dickman (1975b) for example has shown that the ^{13}CO LTE column density can be directly related to the H_2 column density for clouds with visual extinctions $1 < A_v < 10$. Regions of enhanced molecular emission can be the result of: higher optical depth (i.e. higher column density of molecules in a transparent cloud of constant temperature); higher gas temperature (for example in a cloud which is opaque in the CO transition); higher excitation, by collisions with H_2 molecules (i.e. higher space density); or a combination of these effects. Combined observations of isotopic transitions (e.g. the ^{12}CO and ^{13}CO J=1-0 transition) and of molecules with different dipole moments (e.g. the CO J=1-0 and the CS J=3-2 transitions) are needed to disentangle these effects. The general problem of how to interpret radio molecular lines is definitely outside the scope of this review.

Condensed objects, like protostars and MS stars, can be observed in the radio and sub-mm range if they interact with the surrounding interstellar matter. Examples of such interaction are: i) Heating of the surrounding gas, which results in an enhanced line emission; ii) Heating of the grains, which results in an enhanced IR and sub-mm emission; iii) Ionization of the gas, which results both in a free-free continuum and recombination line emission.

In the following, we discuss observations related to a wide variety of objects. We define:
a) *Regions of enhanced molecular line emission or "dense molecular cloud"*: More or less extended regions in an usually much larger molecular cloud, where the CO J=1-0 transition has brightness temperatures > 10 K, where the corresponding ^{13}CO transition is strong and where, usually, mm-lines of molecules with higher dipole moment such as CS, HCN, H_2S and H_2CO are observed in emission.

b) *IR stars*: Unresolved (< 1") objects which emit primary at IR wave-
lengths < 20μ.
c) *Far IR source*: A more extended source spectrum usually can be roughly
approximated by a black-body spectrum with temperatures $\lesssim$ 200 K.
d) *Giant HII region*: Intrinsic flux density $S_5 D^2 \geq$ 400 (f.u.)(Kpc)^2.
e) *Compact HII region*: $10^{-3} < 2r_H^+/pc < 1$; $10^3 < n_e/cm^{-3} < 10^6$;
$10^{-3} < M_{HII}/M_\odot < 10$. An *ionization bounded (ib) compact HII region* is
embedded in a dense shell of neutral gas and dust. A *density bounded (db)
compact HII region* is embedded in an extended low-density HII region.
f) *Radio HII region*: Has peak emission measure $\geq 10^4$ cm^{-6} pc.
g) *C$^+$ region*: C is ionized in a relatively large region (typcially
$\sim$0.5 pc) while the associated H$^+$ region - if observable at all - is much
smaller.
h) *Protostellar shell*: Remnant of the protostellar cloud left behind
after the central star has reached the MS. If an *ib* compact HII region
has formed, the protostellar shell extends from the ionization front to
the edge of the protostellar cloud.
i) *Cocoon*: Dust shell which absorbs radiation and reradiates it at IR
wavelengths.

3) A Possible Evolutionary Sequence of O and B Stars and their Proto-
stellar Shells

    The complexity of the subject warrants a reversal of the usual
procedure; we introduce the review of observations (Sect. II) by out-
lining a working hypothesis for the evolutionary sequence of O and B
stars. This sequence is based on radio and IR observations of the giant
HII region W3 (reviewed by Mezger and Wink, 1974) and on model calcula-
tions of dust-filled protostellar clouds and shells (Yorke and Krügel,
1976, and Yorke (in prep.)). Other papers to be mentioned in this con-
text are those by Wynn-Williams et al (1972), Israel et al (1973), and
Krügel and Mezger (1975) for observations and their interpretation; and
by Davidson and Harwit (1967), Mathews (1969), Larson (1969a, b), Larson
and Starrfield (1971) and Kahn (1974) for model calculations of various
evolutionary stages. On the basis of this possible evolutionary sequence,
we will (Sect. II) tentatively identify observed protostellar objects
with evolutionary stages of protostars of different masses, and we will
estimate the evolution times of these objects.

    We take for granted the existence of a dense molecular cloud in
which a dense blob of some 1 000 $M_\odot$ of gas has condensed. In this blob,
stars from 1 $M_\odot$ upward have formed, and have used up most of the gas.
Close to the center of the newly formed star cluster is a dense proto-
stellar cloud of sufficient mass to form an O or B star. Outside the
star cluster (and in general between the condensations (blobs) of the
large molecular cloud), the gas density is low (some 100 H_2 molecules
cm^{-3}), just enough to thermalize CO. Dynamical calculations by Yorke
and Krügel (1976) start at the time when protostellar clouds of 150 and
50 $M_\odot$ respectively begin to collapse. More recent calculations by Yorke
(in prep.) refer to a protostellar cloud of 20 $M_\odot$. As a result of this
collapse, MS stars of 36, 17 and 12 $M_\odot$ respectively are formed which

correspond to stars of spectral types $\sim$O5-6 to BO. These stars leave be-
hind massive protostellar shells which contain fractions of 76 (66; 40)%
of the mass of the protostellar cloud. At the time of the collapse, the
radii of the protostellar clouds are of the order of 1E18 cm. The compu-
tations by Yorke and Krügel neglect rotation of the protostellar cloud
and magnetic fields and treat the radiation transfer problem only roughly
(diffusion approximation). Furthermore, some of the quantitative results
may depend strongly on the assumed dust model (a mixture of graphite
grains and graphite cores with ice mantles). Nevertheless, the predicted
sequence of evolutionary stages appears to be realistic when compared to
various IR and radio observations. These stages are (values referring to
the 50 $M_\odot$ and 20 $M_\odot$ protostellar clouds are given in paranthesis):

a) 1.5E5 (3.2E5; 4.7E5) yr after the collapse has started and shortly
after a star-like nucleus has formed at the center of the protostellar
cloud, an inner dust cocoon of radius 5E13 (4.5E13; 2.9E13) cm forms.
Inside this cocoon, even refractory graphite grains evaporate. The inner
cocoon would be an IR source of radius 1.6E15 (5.8E14; 3.1E14) cm and
effective temperature 400 (540; 460) K. However, the collapsing proto-
stellar cloud outside the inner cocoon is opaque in the IR. Therefore,
an outside observer will only see an extended far IR source of much lower
color temperature.

b) Radiation pressure from the inner dust cocoon acts on the dust com-
ponent of the infalling material to which the neutral gas is coupled by
friction. Finally, the mass flow is reversed and a second (outer) dust
cocoon forms after 1.6E5 (3.6E5; 6.1E5) yr at a distance of 3E17 (1.E17;
4E16) cm. In the subsequent evolution, both the inner and outer dust co-
coon expand. An outside observer will see the inner cocoon as a hot IR
source (color temperatures 400 to 1 000 K) and the outer cocoon as a
far IR source (color temperature $\stackrel{<}{\sim}$ 200 K). An HII region can only form
inside the inner cocoon and will, in most cases, be unobservable at ra-
dio wavelengths.

c) After 1.9E5 (3.7E5; 6.4E5) yr the inner cocoon becomes optically thin
to near IR and subsequently also to the UV and Lyc radiation. At this
point, quantitative computations stop. During the 1E3 yr in which the
star accretes its final mass of 36 (17; 12) $M_\odot$, a very compact HII re-
gion forms inside the outer cocoon. An outside observer will see this
very compact radio HII region together with the much extended far IR
source formed by the outer cocoon. It is due to the formation of the
outer cocoon by radiation pressure that nearly all far IR sources as-
sociated with compact HII region have the same spectral distribution,
irrespective of the size of the compact HII region (Krügel and Mezger,1975).

d) The compact HII region expands and soon the ionization front will meet
the dust front in the outer cocoon. At this stage, an outside observer
will see both a shell-like HII region and a far IR source of similar
sizes.

e) In the following stages, an *ib* compact HII region will expand inside
the protostellar shell. Its density will decrease while more and more
of the neutral gas is ionized. An outside observer will see a compact
HII region of constant flux density whose turnover frequency moves to-
wards lower frequencies while the integrated IR luminosity decreases.

f) With an expansion velocity of ∿10 km s^{-1}, the ionization front will reach the edge of the protostellar shell in about 3E4 yr. Starting from this point, a *db* compact HII region will evolve, whose total mass stays constant, but whose flux density decreases rapidly (see e.g. Mathews, 1969). It ceases to be a far IR source. The ionization front moves into the region of low gas density which surrounds the protostellar shell and thus forms an extended low-density HII region. The HII region ceases to be a "radio HII region" after the peak emission measure of the *db* compact HII region has decreased to values < 1E4 cm^{-6} pc. Mezger and Smith (1975) estimate an average life time of radio HII regions of ∿5E5 yr.

Similar dynamical computations for smaller protostellar clouds out of which late B stars may form have not yet been made. The evolutionary sequence for an early B star is similar to that described above but with the difference that the compact H$^+$ region is small but is accompanied by a rather conspicuous C$^+$ region. One may safely extrapolate that, for late B stars with lower stellar mass, the mass fraction of the protostellar cloud left behind in the protostellar shell is lower too. This may prevent the formation of an outer cocoon and render the inner cocoon observable. If this picture is correct, early B stars should be visible as IR stars, far IR sources and C$^+$ regions; late B stars may be observable as IR stars only.

In comparing these evolutionary stages with observations, one must be aware that the most severe oversimplification in the model computations is probably the assumption of spherical symmetry of the protostellar shell, which determines the appearance of *ib* compact HII regions and far IR sources. Nevertheless, the following evolutionary time scales for O stars should be realistic:

i) The O star reaches its ZAMS stage after it has accreted the remnants of the inner cocoon and has thus attained its final mass. Only then can the ionization front move freely into the surrounding neutral gas. Thus, a modern theory of HII regions can still use the old fashioned approximation of "immediate turn-on" of the O stars. ii) During about one free-fall time (for O stars, some 1E5 yr) the collapsing protostellar cloud is unobservable. iii) Subsequently, for some 1E4 yr, the protostar is observable as a far and near IR source with no radio counterpart. iv) After the O star has reached its ZAMS stage, a compact HII region forms. Its lifetime as in *ib* HII region lasts typically some 1E4 yr, provided the ionized gas does not reach pressure equilibrium with dense neutral gas. v) The stage of a radio HII region (i.e. the remnants of a *db* compact HII region with peak emission measure 1E4 pc cm^{-6} embedded in an extended low-density HII region) lasts about 5E5 yr. The stage of an optically visible HII region (which requires emission measures ∿ 3E3 cm^{-6} pc) may last over the whole lifetime of an O star, depending on the extent and mass of the associated cloud.

This picture places optically visible HII regions relatively late in the evolutionary sequence of O stars. That is the reason that no sub-section on optical observations of HII regions is included in the following review. Mme Lortet-Zuckermann will report later on optical observations which she feels are relevant to the formation of O stars and compact HII regions.

II. RADIO OBSERVATIONS RELATED TO THE FORMATION OF SINGLE STARS AND
    STAR CLUSTERS

1. Stars Less Massive than O Stars Associated with Dust Clouds

     Dense clouds of interstellar gas which are located sufficiently
close to the sun are seen optically as dark clouds. They are often as-
sociated with T-Tauri stars which are considered to be pre MS stars in
the mass range 0.5 to 2 $M_\odot$ (Herbig, 1962). These may be the regions in
our Galaxy where preferentially low-mass stars form. The CO and ^{13}CO
J=1-O emission from 34 dust clouds has been surveyed by Milman et al
(1975); and from 68 dust clouds by Dickman (1975b). Typical values of the
CO brightness temperature are 10 K; since the CO line is optically thick,
this value is thought to be representative for the kinetic gas temperature
in the clouds. Kinetic temperatures of this order can be maintained in
dense gas clouds by: compressional heating during free-fall collapse; by
ionization of carbon, if enough photons in the range 912 to 1101 A are
available; and by ionization by relatively hard cosmic rays. The latter
source of heating may be the most probable one for extended dust clouds,
especially since ionization of dense interstellar clouds also appears to
play an important role in interstellar gas phase chemistry involving ion
molecules (see, e.g. Herbst and Klemperer, 1976). Milman (1975) finds
enhanced molecular line emission only at the positions of NGC 2023 ,
NGC 2068 and NGC 2024, which are well-known reflection or emission ne-
bulae with exciting stars of spectral type early B to late O. From these
observations and some calculations, Milman concludes that only stars
with relatively strong UV emission (earlier than AO) can heat the sur-
rounding gas by ionization of C and photo-ejection of electrons from
dust grains, but that heating of the gas by collisions with dust grains
(which are heated by absorption of stellar light) is a very inefficient
heating process.

     Herbig (1960) reasoned that massive protostars, whose pre MS con-
traction time is short, should still be closely associated with their
protostellar gas cloud. He selected a number of nearby Ae and Be stars
which, like T-Tauri stars, are closely associated with dust clouds.
Loren et al (1973; for a review of further observations and their inter-
pretation see also Loren, 1975) observed molecular line emission from
dust clouds surrounding these Ae and Be stars and find enhanced CO emis-
sion in every case. CS emission from some of these regions indicates
that they are both hotter and denser than the average cloud. While an
early B star is not hot enough to form a strong H^+ region, it emits suf-
ficient UV photons in the range $912 \leq \lambda/A \leq 1101$ to form an extended C^+
region. It can be observed through its C radio recombination line emis-
sion which, at electron temperatures of ~100 K, is stronger than the
free-free continuum. B stars are also luminous enough to heat the sur-
rounding dust and thus to form a far IR source. This has been observa-
tionally demonstrated for the exciting B1.5 star of NGC 2023 (mentioned
above as a source of enhanced molecular line emission) by Knapp et al
(1975) and Emerson et al (1975). Pankonin and Walmsley (1976) analyzed
its physical state. Both gas and dust temperature decreases from values
of ~100 K close to the star to about 10 K at the edge of the C^+ region

($r_{C^+} \sim 0.5$ pc for an adopted total gas density of 10^4 cm^{-3}). But while
H_2 can exist, at least in the outer part of the C^+ region, CO would be
dissociated in the C^+ region. If this calculation is correct, the C^+ re-
gion can not be the source of enhanced CO emission in the cloud L1630 as
suggested by Milman.

2) The Star Cluster in the Ophiuchus Dark Cloud

     A much investigated example of an optically opaque cloud where a
star cluster is possibly forming deep inside is found in the Ophiuchus
dark cloud. This dust cloud, located at a distance of about 160 pc, ex-
tends over an area of several degrees. In an area of roughly 1.7 x 1.2 pc,
Vrba et al (1975) at $\lambda 2\mu$ observed about 70 stars, most of which do not
have an optical counterpart. The authors arrive at the following con-
clusions: The luminosity function derived for these stars is identical
to that of other young clusters which can be observed optically; the ob-
served IR stars are the brightest members of a star cluster embedded in
a dust cloud; the extinction estimated for the brightest IR stars varies
considerably and is much higher than the average extinction of the cloud,
suggesting the presence of protostellar shells; the extinction law in the
dense cloud is definitely different from the interstellar mean, sugges-
ting the presence of larger size particles, as would be expected if ice-
mantles form around refractory cores. Molecular line emission from the
Ophiuchus dark cloud has been observed by various authors, the most com-
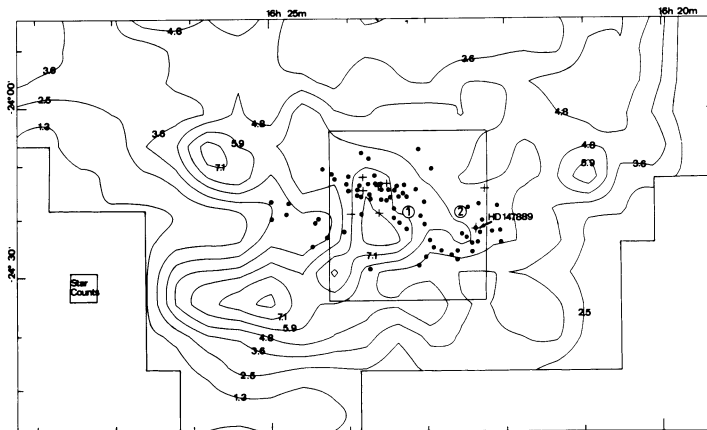

Figure 2: Map of visual extinction in the Ophiuchus
dark cloud determined by star counts (Encrenaz et al,
1975). The curves are labelled by visual extinction,
expressed in magnitudes. The positions of IR stars
(Vrba et al, 1975) are indicated by dots. The corsses
represent continuum sources which could be small com-
pact HII regions. CO observations referr to the rec-
tangle which includes most of the IR stars.

plete investigation being that by Encrenaz et al (1975). Fig. 2 shows
their map of visual extinction, superimposed on which are the IR stars
observed by Vrba et al (1975). These IR stars cover only a small volume
of the much more extended dust cloud. CO and ^{13}CO emission has been map-
ped within the rectangle shown in Fig. 2, which contains most of the IR
stars. The total mass of gas contained within the rectangle (and thus
associated with the main part of the IR star cluster) is estimated to be
$\sim$2 000 $M_\odot$. Figure 3, from a forthcoming paper by Pankonin and Walmsley
(in prep), shows the central part of the IR star cluster. G and VS num-
bers refer to the star lists by Grasdalen et al (1973) and Vrba et al
(1975). C radio recombination lines have first been observed by Brown
et al (1974). The vastly improved C157α results by Pankonin and Walmsley
are shown in Figure 3; the heavy contours refer to the highest and lowest
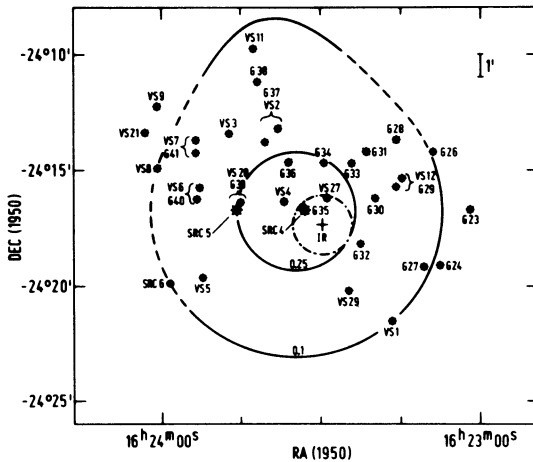observed C157α intensities. Brown and Zuckerman (1975) discovered a num-

Figure 3: Central part of
IR star cluster of Fig. 1
shown together with contour
lines referring to the ob-
served C157 line intensi-
ty (full lines) and far IR
emission (dash-dotted line;
Pankonin and Walmsley, in
prep.). IR stars are la-
belled with VS and G num-
bers, weak continuum radio
sources with SRC numbers.
(For details, see text.)

ber of small continuum sources which they suggest to be weak compact HII
regions; however, more recent λ21 cm observations with the Westerbork
SRT (Encrenaz, priv. comm.) cast some doubt on the reality at least of
the weaker sources. Continuum sources observed by Brown and Zuckerman
are labelled with SRC in Fig. 3. Simon et al (1973) and later Fazio et al
(1976) discovered far IR sources; the strongest far IR source from Fazio
et al is indicated by its dash-dotted half power contour. The density of
the molecular cloud peaks ($n_{H_2} \simeq$ 1E5 cm^{-3}) close to the far IR source.
All these observations appear to be consistent with a star cluster for-
ming deep inside a molecular cloud. The most massive appear to be of spec-
tral type early B, as witnessed by the presence of small compact H$^+$ re-
gions, an extended C$^+$ region and one or more far IR sources. Further, and
consistent with the model calculations by Yorke and Krügel (Sect. I.3),
the massive stars appear to be embedded in circumstellar shells. Accor-
ding to the ideas outlined in Sect. I.1, one might expect that an O star
will form next which would ionize and disperse the remaining gas so that
the star cluster could become visible. While this picture fits in nicely

with the evolutionary sequence of O star clusters outlined in Sect. I,
one should be cautious not to overestimate the reliability of the vari-
ous IR and radio observations on which the picture is based. We are ra-
ther certain that more accurate observations will necessitate modifica-
tions to the picture.

3) O Stars Associated with Molecular Clouds

The association of dense molecular clouds with HII regions is well
known. The number N'_C of Lyc-photons absorbed by the gas is proportional
to the intrinsic radio flux density of the optically thin HII region. If
$N'_C \gtrsim$ 2E48 Lyc-photons s^{-1}, the ionizing star is of spectral type O9 or
earlier. However, the reverse conclusion does not hold, since with in-
creasing gas density more and more Lyc-photons get directly absorbed by
dust grains so that, for densities $\gtrsim$ 1E5 cm^{-3}, the HII region virtually
ceases to exist (Mezger et al, 1974). Or, as outlined in Sect. I.3, in
the pre-ZAMS stage, all Lyc-photons get absorbed by the inner dust co-
coon. Therefore, the total IR luminosity is usually a safer indicator of
the spectral type of a young dust-embedded star and, if $L_{IR} \gtrsim 10^5 L_\odot$, the
object is or will become an O star. The ratio $L_{IR}/N'_C h\nu_\alpha$, i.e. the IR lumi-
nosity expressed in units of the energy available in the form of Lα pho-
tons, is an indicator of the density of dust in the vicinity of the star.
The following discussion relates to HII regions or far IR sources which
are energized by O stars according to the above mentioned criteria for
N'_C and/or L_{IR}. Liszt, in his unpublished thesis (1973; see also Penzias,
1975), presents a consistent set of data which will be referred to in
this paragraph. Liszt mapped the CO and ^{13}CO J=1-0 line emission from 25
clouds associated with HII regions. As far as we can judge, the maps re-
late to regions of enhanced CO emission which represent dense condensa-
tions of gas in a more extended but also more tenuous cloud. (See, as an
example, the discussion of the Orion region in the following paragraph).
All investigated HII regions are associated with such dense clouds. Lower
mass limits range from some 1E2 to 1E3 $M_\odot$ for clouds associated with one
O star cluster; and from some 1E3 to 1E5 $M_\odot$ for clouds associated with
giant HII regions. Liszt finds systematic differences between radial
velocities of HII regions and molecular clouds: v_{LSR}(H109α) $-v_{LSR}$(CO) is
negative for visible HII regions and positive for obscured HII regions.
Liszt interprets this as an indication that, similar to the situation in
Orion A (see following sub-section), HII regions are often ionization
bounded in one direction (where the ionization front hits a dense neutral
gas) but density bounded in other directions, where the ionized gas can
freely expand. However, the validity of Liszt's statistics is question-
able since many of his "obscured" HII regions are so remote that obscura-
tion due to dust along the line of sight is more probable than obscuration
by the molecular cloud itself.

Out of 60 Sharpless HII regions, Blair et al (1975) detected CO emis-
sion from associated molecular clouds in 30. Many of these optically vis-
ible HII regions relate to relatively late stages of their ionizing stars
(Sect. I.3). The presence of CO clouds indicates that not all HII regions
may be able to disperse the remnants of their parent clouds during their
MS lifetimes.

4) The Orion Region: Star Formation in an Interarm Cloud Complex

        The Orion region is a well investigated example of an OB-star asso-
ciation, a compact HII region, and a dense molecular cloud, where the op-
tically visible sub-groups of the association are in various evolutionary
stages and where inside a dense condensation of gas, O and B stars form.

Figure 4: ^{13}CO map of
the dense Orion mole-
cular cloud, superim-
posed on a photograph
showing Orion A (=M42+
M43) south of the cloud
and NGC 1973, 5, 7
north of the cloud.
(Kutner et al, 1976).

The Orion region is obviously not part of the main spiral structure of
our Galaxy (see Fig. 1) and therefore maybe representative of O star
formation in the interarm region. Figure 4 shows a ^{13}CO map of the Orion
molecular cloud proper, a dense ($n_{H_2} \sim 5E4$ cm^{-3}) cloud containing ~ 2 000 M$_\odot$
of gas (Kutner et al, 1976). The optically visible OB association ex-
tends $\sim 12^\circ$ from the molecular cloud to the north-west. It consists of four
discernable sub-groups which differ in age by at least 1E7 yr (Blaauw,
1964). An extended region of weak CO emission extends from the molecular
cloud over $\sim 5^\circ$ to the south-east (Kutner et al, in prep.). OB association
and extended molecular cloud run approximately parallel to the galactic
plane. The dense molecular cloud runs about perpendicular to the galactic
plane; it is located at the interface between OB association and extended
cloud. At its southern end is located the compact HII region Orion A
(which comprises M42 and M43) at the northern end is located the HII re-
gion NGC 1977. The southern and northern maxima in the ^{13}CO map (Fig. 4)
are referred to as OMC1 and OMC2. OMC1 has a high density core ($n_{H_2} \gtrsim$
2E6 cm^{-3}) which comprises 200 M$_\odot$; OMC2 has a similar core, but less dense
and massive. Orion A, OMC1 and OMC2 are far IR sources; the former two
have luminosities of 1E5 L$_\odot$ which are typical for O-stars, while the IR
luminosity of OMC2 is about a factor of a hundred less. The far IR source
associated with Orion A is extended and correlates well with the free-free
emission. The far IR sources associated with OMC1 and OMC2 are much nar-
rower ($\lesssim 1'$). The far IR source associacted with OMC1 is known as the
Kleinmann-Low (KL) nebula, which comprises the Becklin-Neugebauer (BN) IR
star (of color temperature ~ 600 K) and a cluster of less luminous IR stars
(Wynn-Williams and Becklin, 1974); similarly, a cluster of IR stars is lo-
cated inside the far IR source associated with OMC2 (Gatley et al, 1974).

$\lambda 1$ mm emission from somewhat cooler dust grains is observed over a region $\sim 7'$ centered on OMC1 (Harvey et al, 1974) and at the peak of OMC2 (Hudson and Soifer, 1976). Various observational arguments suggest that Orion A is ionization bounded on its rear side where the ionization front hits a dense molecular cloud, but is density bounded in other directions (see the review by Zuckerman, 1975, Lect. Notes Phys. 42, p360)[*].

Are the Trapezium cluster and the IR star clusters separate sub-groups? To answer this question let us tentatively identify: i) Orion A as a db compact HII region. ii) The BN-KL IR complex as a late O star in a stage where both inner and outer dust cocoon are observable. This interpretation is supported by the recent detection of Brackett α emission from the vicinity of the BN star, indicating the presence of a very compact HII region ($n_e \gtrsim 3E5$ cm^{-3}; $r_{H^+} \lesssim 5E14$ cm), such as one expects to form inside the inner dust cocoon (Grasdalen, 1976). iii) The IR stars in OMC2, we identify as a star cluster where stars up to late B have formed. We then conclude, on the basis of the evolutionary time scale estimated in Sect. I.3, that the evolutionary ages of these OB stars differ by probably less than 1E5 yr; and that some 10^5 yr from now, the whole complex of stars associated with the dense Orion molecular cloud may be seen as one sub-group of the Orion association. This implies that O and B stars form within a short time interval in different parts of a sub-group; that therefore the ionization front of a db compact component is bound to interact with dense, neutral protostellar clouds of less evolved O and B stars; and that the actual units of star formation may be smaller than a sub-group (which, according to Blaauw, 1964, contains $\sim 2\,000\,M_\odot$ of stars) and may rather be represented by IR star clusters like those observed in OMC1 and OMC2.

In summary, the following picture emerges for the formation of OB stars in the Orion complex; it may be typical for all large cloud complexes in the interarm region: Formation of O stars started at least 1E7 yr ago in the north-western corner of a molecular cloud which then extended over 20°. Subsequently, the formation of OB stars proceeded in the direction of the Trapezium cluster, where O stars have formed recently. At present, OB stars close to the ZAMS are found in OMC1 and OMC2. This picture suggests that formation of O stars will proceed further, into the molecular cloud which extends to the south-east of the Trapezium. Star formation and subsequent dispersion of the remaining gas in the OB association must have been rather efficient, since no CO emission is detected there (Tucker, priv. comm. quoting observations made by G. Chin). What created the dense molecular clouds out of which OB stars and star clusters can form? We do not know. But one may visualize a compression wave moving across an extended molecular cloud with a speed of ~ 100 pc/10^7 yr $\simeq 10$ km s^{-1}, which creates the dense clouds and thus initiates star formation. Expanding HII regions and supernovae may play a role in driving this compression wave.

----

[*] A symposium on HII regions and related topics, which summarizes radio and IR observations of HII regions up to 1974 was held in Mittelberg, Austria, January 1975. The proceedings of this symposium are published will be referred to as above. See ref. Lect. Notes Phys. 42.

5) W3:Formation of O Stars in Main Spiral Arms

Giant HII regions require more than one early O star to account for their ionization. Giant HII regions define the main spiral arms in external galaxies. In our Galaxy, all observed giant HII regions can be accounted for as being located in four main spiral arms (see Fig. 1) and in the central part of the nuclear disk. Many giant HII regions have been observed in the radio range with an angular resolution of a few arc sec with synthesis radio telescopes. A full account of these observations up to early 1976 is given in Table 2 of Mezger and Wink (1976). With a few exceptions (all very remote giant HII regions such as W49 or GO.7-O.O), it is found that all giant HII regions can be resolved into compact components (sometimes superimposed on an extended background of low surface brightness) where each compact component could be ionized by one single early O star. This suggests that giant HII regions represent OB star associations which are composed of a number of subgroups similar to the Orion OB association discussed in the previous paragraph. The main difference between OB associations forming in cloud complexes in the interarm region and those forming in main (density wave) spiral arms being that, in main spiral arm OB associations, a large number of O stars reach the MS nearly at the same time while, in interarm OB associations, there is a rather long time delay (of the order of the MS lifetime of O stars) between the formation of O stars in adjacent subgroups.

The optically obscured HII region W3 is part of a giant complex of HII regions located in the Perseus arm at a distance of ∿3 Kpc from the sun and ∿12 Kpc from the galactic center. This complex also includes the optically visible HII regions IC1848, IC1805 and IC1795. A radio map of this region obtained at $\lambda 11$ cm with an angular resolution of ∿11' by Wendker and Altenhoff (in prep.) is shown in Fig. 5. IC1805, IC1795 and W3 appear to form one OB association where the age of the O stars (referred to ZAMS) decreases from < 5E5 yr at the eastern edge to zero in
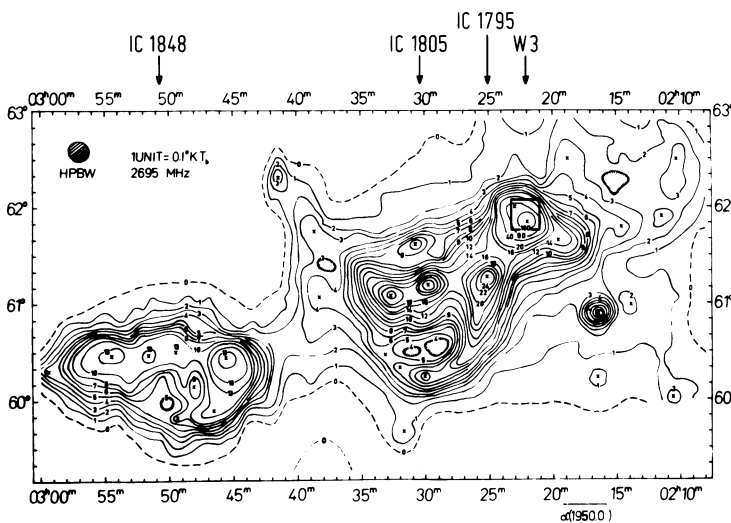

Figure 5: Contour map of IC1848, 1805, 1795 and W3 observed at $\lambda 11$cm with an angular resolution of 11' (Wendker and Altenhoff, in prep.). The rectangle indicates the synthesized area shown in Fig. 5.

the compact objects in W3. The intrinsic flux density is $S_{2.7}$ (IC1805 + IC1795 + W3) x D(= 3 Kpc)^2 = 3 600 (f.u.)(Kpc)^2 (Wendker and Altenhoff, in prep.), i.e. 36 times the intrinsic flux density of the Orion Nebula. (This is a lower limit since IC1805 and IC1795 appear to be density boun-ded to a large extent.)

In the context of star formation in main spiral arms, W3 appears to be of most interest. Fig. 6, from Sullivan and Downes (1973), is an over-lay on a Palomar red print of an aperture synthesis map of W3 (angular resolution 25" x 28"; the synthesized area is shown in Fig. 5 by a solid

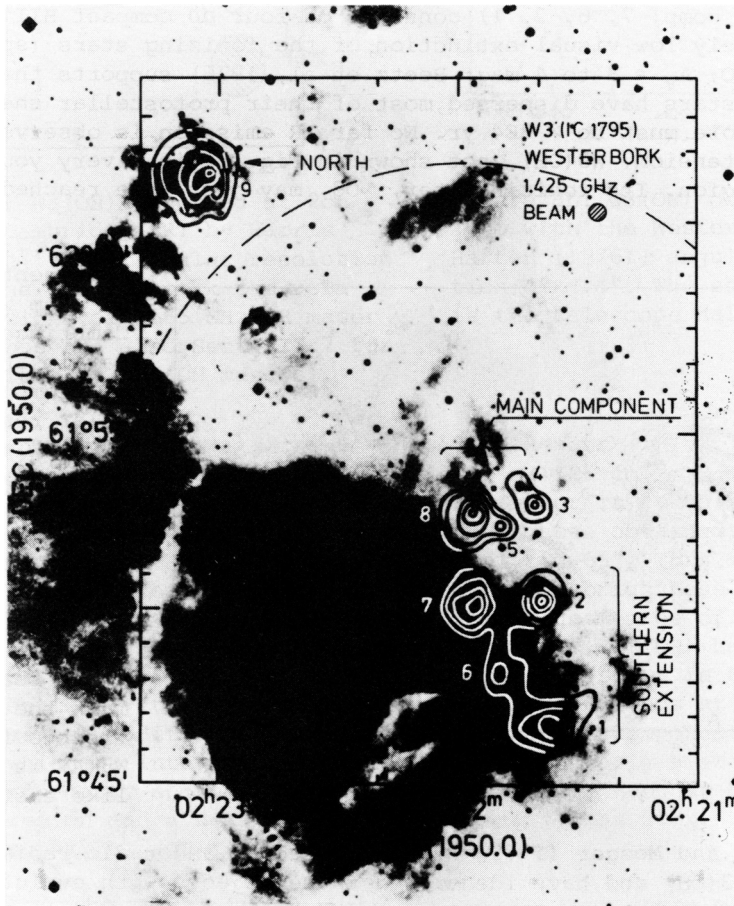Figure 6: W3, Main component, Southern extension and Northern component observed at $\lambda 21$cm with the Wester-bork SRT. Resolution 25"x28" (Sullivan and Downes, 1973). Compact HII regions 3,4,5 and 8 are part of the Main com-ponent; 1,2,6 and 7 are part of the Southern extension. W3(OH) is located 17' southeast of the Main component and outside the synthesized area.

rectangle). About 17' south-east of W3, main component, and outside the
synthesized map is W3(OH), one of the most compact HII regions observed
to date. For the following discussion, we refer to Mezger and Wink (1974;
and 1975, Lect. Notes Phys. 42, p. 408). Only more recent results will be
referenced explicitly.

In W3, we recognize four regions of OB star formation. W3(north)
(= comp. 9 in Fig. 6), a *db* compact HII region, is ionized by a late
O star of age (counted from ZAMS) $\sim$3E4 yr. W3(main component) (= comp. 8,
5, 4, 3) contains seven OB stars. Even the most evolved HII region, W3(A),
is still ionization bounded and sourrounded by its protostellar shell.
Ages of ionizing stars therefore range from O to $\lesssim$ 3E5 yr. W3(southern ex-
tension) (= comp. 7, 6, 2, 1) consists of four *db* compact HII regions.
The relatively low visual extinction of the ionizing stars (spectral type
BO or late O; A_V = 8 to 4 mag; Beetz et al, 1976) supports the conclusion
that these stars have dispersed most of their protostellar shells. Their
ages therefore must be > 3E4 yr. No far IR emission is observed from the
southern extension. W3(OH), not shown in Fig. 6, is a very young *ib* com-
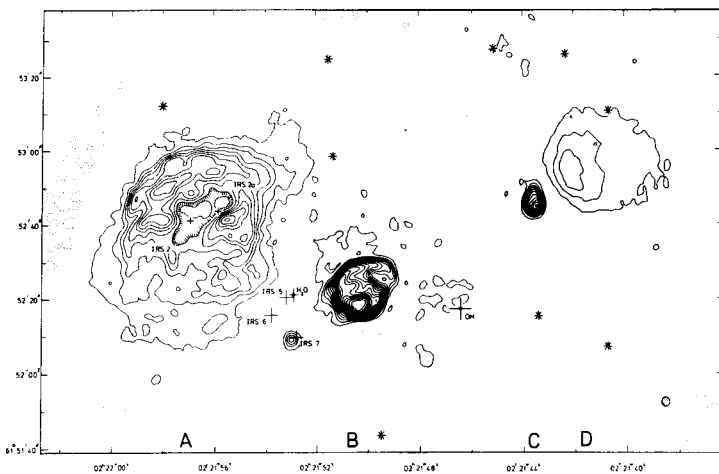pact HII region. Its ionizing star, $\sim$O8, may just have reached the MS.

Figure 7: W3(main
component) observed
at λ6cm with the
Cambridge SRT by
Harris and Wynn-
Williams (1976); an-
gular resolution
2"x2.3". Crosses
mark the positions
of IR stars and cros-
ses with dots in the
center mark positions
of OH and H_2O masers.
The shaded ellipse is
the half-power tele-
scope beam. Asteriks
mark the positions of
visible field stars.
W3(A) is the shell-
like eastern component.

Krügel and Mezger (1975) have analysed IR and radio radiation from
W3(A) and W3(OH) and have identified these objects with evolutionary stages
of O stars described in Sect. I.3.c) (W3(OH)) and d) (W3(A)) respectively.
Harris and Wynn-Williams (1976) at 5 GHz made an aperture synthesis map
of W3(main component) with an angular resolution of 2" x 2.3" which is
shown in Fig. 7. The main ionizing star of the shell-like eastern HII
region W3(A) is IRS2; a somewhat less luminous star, IRS2a, has been de-
tected in the near IR by Beetz et al (1974), at a projected distance of
2E17 cm from IRS2. All HII regions shown in Figure 7 appear to be ion-
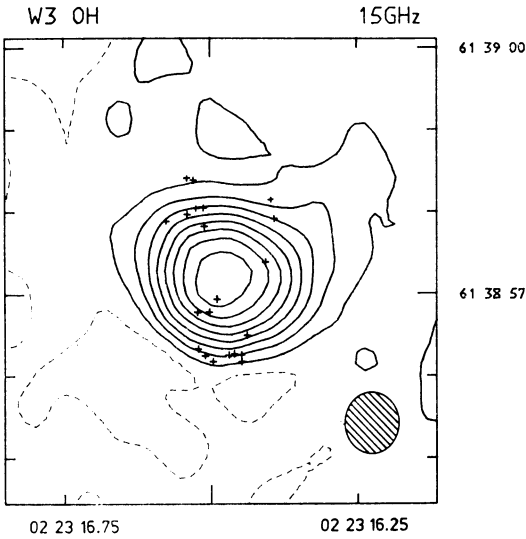ization bounded.

W3 OH   15GHz

Figure 8a: W3(OH) observed at 2cm with the Cambridge SRT by Harris and Scott (1976); angular resolution ∿0.65". The crosses mark the relative positions of 1665 MHz OH maser sources (but see also Sect. II.7 for the positions of the OH masers).
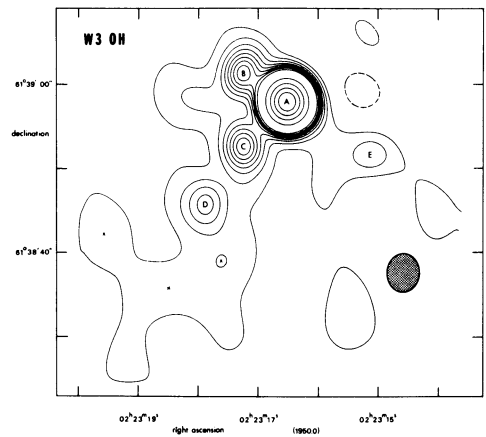
Figure 8b: W3(OH) observed at λ6cm with the Westerbork SRT by Harten (1976); angular resolution 4"x4.4". The shaded ellipse is the telescope half-power beam.

According to the analysis by Krügel and Mezger (1975), W3(OH) consists of a compact HII region ($r_H + \sim 4E16$ cm; $n_e \sim 1E5$ cm^{-3}; $M_H +/M_\odot \sim 4E-3$), which is embedded in a dust cocoon whose diameter is 10 to 20 times larger. Recently, at 15 GHz, a map of W3(OH) has been obtained by Harris and Scott (1976) with an angular resolution of 0.65". This map is shown in Fig. 8a. Although some structure is seen, the brightness distribution of the free-free emission still shows a very high degree of symmetry. At 5 GHz and with an angular resolution of 4" x 4.4", W3(OH) has been mapped by Harten (1976). Besides the main component (shown in Fig. 8a) which is still optically thick at this frequency, Harten finds at least four, possibly seven, additional but much weaker compact components (shown in Fig. 8b) which he interprets as being ionized by early B stars. About 6' to the north-east, another, more evolved B star is seen as both a *db* compact HII region and a weak far IR source (Mezger and Wink, 1975, Lect. Notes Phys. 42, p. 408).

Liszt (1973) observed enhanced CO emission from dense clouds associated with W3(main component) and W3(OH) for which he estimates lower mass limits of $2E3$ $M_\odot$ and $9E2$ $M_\odot$, respectively. The H56α line of W3(OH) has been detected by Hughes and Viner (1976). Its radial velocity V_{LSR} (H56α) is -54 km s^{-1} and thus differs by -7 km s^{-1} from the radial velocity of the CO cloud, v_{LSR} (CO) = -47 km s^{-1}, (Liszt, 1973). Not much is known about a more extended cloud of lower density which may encompass all four regions of OB star association. Preliminary CO observations appear to show that such a low-density cloud is present in those regions where the

HII regions are obscured by dust (see Fig. 6), while CO emission disappears in regions of Hα emission (Thaddeus; Lada, priv. comm).

What can we learn about star formation in OB associations in main spiral arms? A comparison with the Orion region shows a number of correspondences but also some basic differences: The optically visible HII regions IC1848/1805/1795 can be compared to the subgroups in the Orion OB association, except that there appear to be many more subgroups whose ages probably differ by less than 5E5 yr. *db* compact HII regions such as W3(north) and W3(southern extension) can be compared to Orion A and NGC 1977. *ib* compact HII regions and IR sources without radio counter part in W3(main component) and W3(OH), which are embedded in dense molecular clouds, can be compared to OMC1 and OMC2. Again the number of OB stars close to or on the ZAMS is much larger in W3. There appears to exist a low density CO cloud which encompasses the four regions of OB star formation in W3. It would be highly interesting to know if a low density CO cloud similar to that in the Orion region extends to the west of W3, approximately parallel to the galactic plane. This comparison supports our introductory statement that giant HII regions represent OB associations in main spiral arms. The basic differences are the much larger number of subgroups and their much narrower age spread in the main spiral arm OB association. In the Orion region, it appears that a compression wave proceeds from west to east, creating the physical conditions necessary for the formation of OB stars. In IC1848/1805/1795/W3 there appears to be a systematic decrease in evolutionary ages of the compact HII regions from east to west. However, whatever creates physical conditions for OB star formation in W3 (such as, for example, compression of the gas in the shock front of a density wave spiral arm) acts on a much global basis and appears to create more compact OB associations, i.e. the number of OB stars per unit volume appears to be higher.

6) Other HII Regions: A Review of Reviews

Further reviews of observations related to the association of compact or giant HII regions, IR sources and molecular clouds are given in the proceedings of the Mittelberg symposium (1975, Lect. Notes Phys. 42) by D. Lemke for M17, S. Harris for DR 21, T. L. Wilson for W49, J. Bieging for W51 and a summary by A. H. M. Martin for Sgr B2. The association of ionized gas, IR sources and molecular clouds in the galactic center region have been reviewed by Mezger (1974) and Downes (1974). Other recent papers which are of interest in the context of star formation are those by Chaisson and Willson (1975) on M2O, by Lada et al (1976a) on M8 and Lada (1976) and Lada et al (1976b) on M17, and by Israel (1976) on W58, a complex of extended and compact HII regions (which include K3-5O), located in the Perseus arm at a distance of ∿9 Kpc from the sun. The paper by Israel especially supports the picture that conditions for the formation of O stars move from the edge of a cloud towards its center. The detection of an extended (85 x 22 pc) molecular cloud of intermediate density ($n_{H_2} \simeq$ 5E2 cm^{-3}) associated with M17 (Elmegreen and Lada, 1976) supports our conclusions in Sect. II, 4 and 5 that OB associations form out of extended molecular clouds but the O stars will only form in those parts of the cloud where gas densities are one or two orders of magnitude higher than the average cloud density. It further confirms that parent

clouds out of which OB associations form preferentially extend parallel
to the galactic plane. Special attention should be given to the review
paper by Habing (1975, Lect. Notes Phys., p. 156) on compact HII regions,
in which he analyzes primarily Westerbork synthesis observations of ga-
lactic HII regions. The true compact HII regions (which are centrally
ionized) can be divided in those whose density decreases from the center
outward; and those which show a shell-like structure. In the light of
our discussion in Sect. I.3, these two classes of compact HII regions
are related to different evolutionary stages of protostellar shells. Be-
sides these two genuine classes of compact HII regions, Habing finds an-
other type of high-density HII region which is the result of an interac-
tion of an ionization front with a dense cloud of interstellar matter.
Orion A (Sect. II.4) is the most famous example of such an interaction.

   Radio observations of HII regions have recently been reviewed by
Mezger and Wink (1976) with special attention being given to high reso-
lution observations with single dish telescopes at high frequencies and
with synthesis radio telescopes. It appears that the largest ib compact
HII regions have sizes $\simeq$ 2E18 cm while db compact HII regions have sizes
$\gtrsim$ 2E18 cm. Such a transition point from ib to db compact HII regions
should occur when the ionization front reaches the edge of the proto-
stellar cloud (Stage f in the evolutionary sequence outlined in Sect. I.3).
A radius of 1E18 cm for the protostellar cloud agrees well with the ini-
tial conditions for the collapsing protostellar cloud in the dynamical
computations by Yorke and Krügel (1976). The observed masses of ionized
gas in compact HII regions $M_{HII} \lesssim$ 10 $M_\odot$, however, are smaller than the
masses left over in the protostellar shells of their models. This dis-
crepancy could be due to the fact that dense fragments of the protostel-
lar shell remain neutral. In fact, there is mounting evidence of a high
degree of clumping of the ionized gas. The size distribution of these
hypothetical clumps has not yet been directly observed. But recent aper-
ture synthesis observations of Orion A by Gull and Martin (1975, Lect.
Notes Phys. 42, p. 369) obtained with an angular resolution of 7.5" x 20"
show that about 40% of the total flux density (but not of the mass of
ionized gas) contained in the synthesized region is contained in struc-
ture of angular size < 1.3' corresponding to linear sizes < 5E17 cm. Most
of this fine structure appears to be unresolved, corresponding to linear
sizes $\lesssim$ 8E16 cm. This result may have some bearing on the problem of frag-
mentation of a protocluster.

   Not much information has been obtained relating to the process of
star formation in the galactic center region, although a wealth of radio
and IR observations have been published. The Sgr B2 molecular cloud, with
a total mass of 3E6 $M_\odot$, is probably the most massive cloud known in the
Galaxy (Scoville et al, 1975) and, in the giant HII regions GO.7-O.O and
GO.5-O.1 which are associated with this cloud, formation of O stars oc-
curs at an extremely high rate. The nucleus of the Galaxy is surrounded
by very massive compact HII region Sgr A West ($n_e \sim$ 1.4E3 cm^{-3}, $M_{H^+}/M_\odot \sim$6E3).
The nature of the source of ionization of Sgr A West is still not yet un-
derstood.

7) Molecular Masers and Star Formation

In 1965 OH maser sources were discovered. In 1967 it became clear that class I OH masers and compact HII regions are closely associated in space. Class I masers emit primarily in the central 1665 and 1667 MHz OH lines, which are highly polarized. In 1969 H_2O masers were detected, again in regions of active star formation. The OH and H_2O masers occur as clusters of emitters, each of which exhibits a narrow line of width $\lesssim$ 1 km s^{-1}, apparent sizes of 1E13 to 1E14 cm in size, and has brightness temperatures from 1E13 to 1E15 K. The cluster of emitters covers a region 1E16 to 1E17 cm in size. The H_2O masers change their intensities in time scales of months. Since the discovery of molecular masers, vast efforts by both observers and theorists have been made to explain this phenomenon. Nevertheless, the physical state of the gas in molecular maser sources is only known within rather wide upper and lower limits (say 1E6 to 1E11 cm^{-3} for the density and 20 to 1 000 K for the kinetic temperature). And the number of proposed pumping models has been reduced by elimination of the physically improbable models rather than by observational verification of predictions made. A review of molecular masers is outside the scope of this paper (but we would like to draw attention to the excellent review paper by Strel'nitskii, 1975). In this section, we are concerned with one specific aspect: What can observations of molecular masers tell about star formation?

What is the relation between OH/H_2O masers and massive protostars or ZAMS stars? The association of OH and (probably db) compact HII region has been investigated by Habing et al (1974) who conclude that many, and probably all, class I OH masers occur near OB stars on, or close to, the ZAMS. These authors also suggest that the OH maser phenomena disappears when the db compact HII region has expanded to sizes $\gtrsim$ 2E17, implying a lifetime of $\lesssim$ 1E4 yr. At this distance, densities in the protstellar shells in Yorke and Krügel's models attain values $n_{H_2} \sim$ 1E5 cm^{-3}. If OH masers require gas densities $\gtrsim$ 1E6 cm^{-3}, their disappearance at this stage could be easily explained. According to Winnberg (priv. comm), to date 14 out of 18 class I OH masers (where both positions of maser sources and of compact HII regions have been measured with interferometers) coincide with compact HII regions with an rms uncertainty of $\sim$1".

The association of H_2O masers with OH masers and with other protostellar objects or ZAMS stars has been investigated by Lo (1974; see also the review by Burke, 1975, Lect. Notes Phys. 42, p. 188; and Lo et al, 1975a). He finds that H_2O masers - like OH masers - are found in regions of active OB star formation; but that H_2O masers - unlike OH masers - are either not associated with compact HII regions or, if they are associated, their positions do not coincide. On the basis of this coincidence or lack of coincidence, together with the observational or circumstantial evidence for quite different dynamical time scales of H_2O and OH masers (see above), Lo suggests that H_2O masers represent an earlier evolutionary stage of massive protostars which occurs prior to the formation of db compact HII regions. Recent simultaneous VLBI observations of OH/H_2O masers by Mader et al (1975) in W3(OH) and W49N support this picture. Their result for W3(OH) is shown in Fig. 8. The two clusters

of OH/H_2O emitters are distinctly separated by a projected distance of
∿3.4E17 cm (for D = 3 Kpc). Comparison with accurate interferometer po-
sitions of the OH masers (Welsh, priv. comm.) shows that the OH maser is
associated with the *ib* compact HII region but that the cluster of OH emit-
ters lies at its western edge (and not surrounding it as suggested in
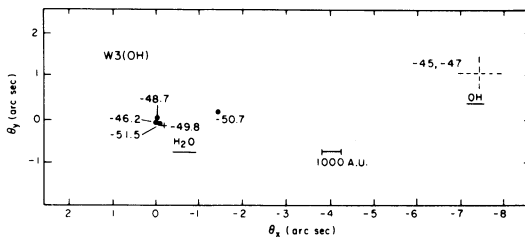Fig. 8a) while the H_2O maser has no radio or IR counterpart.

Figure 9: Relative positions of the OH and H_2O masers in W3(OH) derived by Mader et al (1975). The indicated OH position is a mean position for the blended features between -45 and 47km s^{-1}.

Burdjuzha et al (1975, Lect. Notes Phys. 42, p. 195) suggest a somewhat
different (and, in the light of recent observations, less probable) model
where, in *ib* compact HII regions, H_2O masers are located in the transition
zone HII-HI, while OH masers are located farther out in the protostellar
shell between ionization front and preceeding shock front.

The pattern of circular polarization observed in OH masers can be
interpreted as Zeeman splitting; this yields magnetic fields of typically
a few mG (Davies, 1974). More recent observations by Lo et al (1975b) yield
6 mG for W3(OH). Zeeman splitting of the λ21 cm hyperfine structure line
suggests a general magnetic field of 2μG in clouds of density n_H ∿1 cm^{-3}.
If this field is frozen into the gas, its field strength must increase
∝ n_H^α with α < 2/3 (see Mestel, this volume). Magnetic fields derived for
other OH masers are similar. They are compatible with densities ∿1E6 cm^{-3}
estimated on the basis of realistic pumping models of OH masers.

A third class of masers detected in 1974 by Snyder and Buhl occurs
in the rotational transitions J = 1→0, and 2→1 of the first vibrational
state (v = 1) of the SiO molecule. SiO masers appear generally to be as-
sociated with late type (M3 - M9) Mira variables. No SiO masers are as-
sociated with OH/H_2O/IR sources in, or close to, HII regions, with the
only exception of an SiO maser observed in the direction of the KL nebula
in the Orion region (Snyder and Buhl, 1975).

In summary: Both H_2O and OH masers appear to occur in massive proto-
stars and protostellar shells. H_2O masers probably have gas densities of
∿1E9 cm^{-3} and kinetic temperatures of ∿1E3 K; they occur before a compact
HII region forms. In the evolutionary sequence outlined in Sect. I.3, the
H_2O maser phenomenon would be compatible with the evolutionary stages a)
and b), with the emitting regions located close to the inner dust cocoon.
Densities and temperatures in OH masers are probably considerably lower,
say ∿1E6 cm^{-3} and∿1E2 K; they occur when *db* compact HII regions have for-
med and would be compatible with stages d) and e), with the emitting re-
gions being located just outside the ionization front. Although not much
information related to the physical state of the gas can be deduced, H_2O
masers especially may be the earliest observational manifestation of a

pre O star. SiO masers appear to be associated with late type stars in post MS evolutionary stages and thus are not of much interest in the context of star formation, but may be helpful to discriminate between pre MS and post MS objects.

III. STAR FORMATION RATES IN THE GALAXY

1) As a Function of Density

Radio observations of giant HII regions can be used to determine the rate of star formation (Mezger & Smith, 1975, hereafter referred to as MS). Detection of giant HII regions is nearly complete for our half of the Galaxy, and the number of Lyman continuum photons needed for their ionization can be calculated. If the initial mass function (IMF) is constant over the Galaxy, the photon rate is proportional to the star formation rate. MS derived the rate as a function of distance from the Galactic center; the total value was 4 $M_\odot$/year throughout the Galaxy derived from a total photon flux in giant HII regions of 48 10^{51} sec^{-1}.

The star formation rate is, a priori, expected to be a function of many parameters: amount of gas available, metal abundance, strength of shock waves, and probably others. The parameter which has been singled out in the past for the most attention is the gas density, ρ. Schmidt (1959) favoured a dependence on ρ^2; however, none of the arguments he used at that time remain valid.

An apparently straight forward way to determine the exponent of such a law has been used by Emerson (1974) and by Madore et al (1974); earlier attempts are referenced by the latter. They plot HI column densities versus blue star counts or HII region counts (indicators of star formation). Both encountered difficulties. Emerson (whose results cover the region of greatest HI density in M31) noted that young and old OB associations and HII regions produce different results. Madore et al noted that the inner and outer regions of M33 give different results.

There are several aspects to be noted about the above experiments: 1. They do not allow for the presence of molecular H, now known to account for most of the gas in our own Galaxy; 2. They use column densities rather than volume densities; 3. They use data from different regions of the galaxy.

For comparison with the work of Emerson and of Madore et al, we plot in Fig. 10 log N_C versus log (M_{gas}) for our own Galaxy from Smith, Biermann & Mezger (in preparation, hereafter referred to as SBM). N_C is the number of Lyman continuum photons absorbed in giant HII regions, and includes a correction for absorption by dust inside the HII region. M_{gas} includes an estimate of the molecular H density from CO observations (ranging from 80% of the gas at 5 Kpc from the center to 50% at 10 Kpc); somewhat better estimates can probably be made with more recent CO studies (Gordon and Burton, 1976). Both quantities plotted are surface densities averaged over annuli in the galactic plane. The gas between 4 and
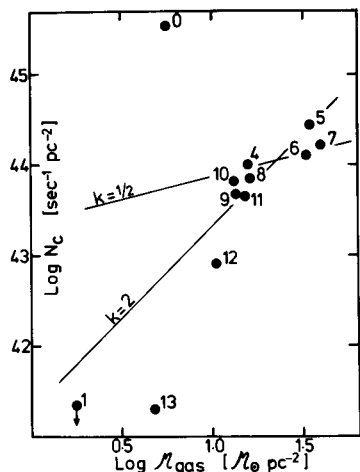
Figure 10: Plot of Log N_C versus Log M_{gas} for annuli in the Galaxy. The points are labelled with the inner radius limit. The lines indicate slopes of 1/2 and 2.

13 Kpc is mostly H_2, for which the scale height is ~ 70 pc out to 8 Kpc and may then increase very slowly. Changes in mean density of the gas appear to reflect changes in numbers of clouds, not changes of the density or size of the clouds. Thus, we expect the total amount of gas available, rather than the mean volume density, to be the more physically relevant parameter.

The problem with this method of determining the slope is made reasonable clear by Fig. 10. Between 4 and 12 Kpc, the main spiral arms, the most gas and the most star formation occur; the observed points do not cover a sufficient range to define a slope. Within this area, a common law between star formation and density might be expected to apply because the process in all spiral arms is qualitatively similar. However, the metal abundance probably varies and the strengths of the shock fronts on the inner edges of the spiral arms (presumably a critical parameter (Woodward, 1976)) varies in strength with distance from the center. Thus the amount of gas is probably not the most important factor that changes from one annulus to another.

In the galactic center, the rate of star formation is probably controlled by different factors, as must also be the case in all regions <4 and >12 Kpc from the center, outside the region of main spiral structure. The galactic center point falls 2 orders of magnitude higher than is compatible with any simple relation; the other points fall far below. We conclude that there is little support for a common law representing the star formation rate at different positions in the Galaxy.

2) As a Function of Time

We now apply a different approach. We look for the dependence of the star formation rate on time, and use the surface density of gas as a parameter. The surface density is probably a good parameter in as much as the amount of gas remaining in a given annulus (assumed isolated from all others) is probably monotonically related to the time and to the metal enrichment, while the strength of the spiral shock wave probably does not change much with time.

We express the relation in the form $dM_*/dt \propto (M_{gas})^k$. To demonstrate the nature of the problem, we give the analytical solution for k=1. We assume instantaneous recycling. i.e. a fraction r of the gas going into stars. dM_*, is returned immediately to the interstellar medium. Hence, the total mass, $M_{tot}=(1-r)M_*+M_{gas}$. We find, (for solutions of this as well as the general case, see Audouze et al, 1975):

$$M_{gas}/M_{tot} = \exp (-t/\tau) \qquad\qquad (1)$$

$$dM_*/dt = M_{gas}/\tau(1-r) \qquad\qquad (2)$$

Thus, given M_{gas}/M_{tot} at the present time $t = 1.4 \ 10^{10}$ yr, we may calculate τ, the rate constant and then predict the present value of dM_*/dt. This is to be compared with the observed value. MS made this comparison and found reasonable agreement between the k=1 analytical solution and the observed rates averaged over annuli in the Galaxy. They assumed a Salpeter (1955) initial luminosity function and the corresponding stellar values from Mezger et al (1974).

Both 'observed' and predicted star formation rates depend on the adopted IMF. The IMF is commonly derived from star counts in the solar neighbourhood. In order to relate the function for stars > 2 $M_\odot$ (with ages much less than the age of the Galaxy) to that for low mass stars, one makes an assumption about the rate of star formation over the life-time of the Galaxy. Salpeter assumed a constant rate of star formation and arrived at an IMF that is well represented by a power law with an exponent -1.35. However, if one allows for some dependence on the amount of gas available (or any other function that decreases with time), the derived IMF for stars < 0.8 $M_\odot$ is greatly reduced. Fig. 11 shows the derived curves for a rate dependent on $(M_{gas})^k$ where k is O (the Salpeter function) O.5,1 or 2. (Curves of this type were first derived and discussed by Schmidt (1963, but see also 1959)).
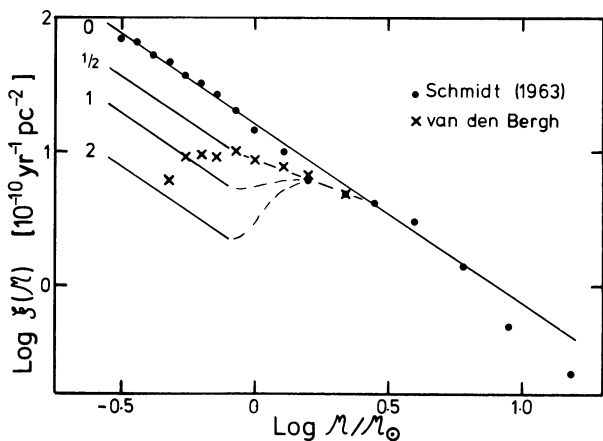

Figure 11: The initial mass function (IMF) derived from star counts in the solar neighbourhood for a star formation rate proportional to $(M_{gas})^k$. The dots are from star counts and the M_V-M relation tabulated by Schmidt (1963) and an age of the Galaxy of 1.4 10^{10} years. Crosses are van den Bergh's (1961) cluster function, converted to an IMF with the same M_V-M scale.

Thus, one must be selfconsistent and use an IMF that corresponds to the same value of k for both. Increasing k has three consequences:
1. The mass of stars associated with a given number of photons decreases, so the observed star formation rate decreases.
2. The 'return rate' is higher, so the predicted star formation rate increases.
3. The rate of star formation in the past relative to the present is increased - which causes the predicted present rates to decrease.

The results are sensitive to the cut-offs of the IMF. The results presented here are for an IMF truncated at 0.1 and 85 $M_\odot$ the lower cut off may be unrealistically large.

Fig. 12 shows the 'observed' rates for k=1/2. The conversion factor from photon rate is 1.175 $\langle M \rangle / \langle N_C \rangle$ t(HII), where $\langle M \rangle / \langle N_C \rangle$ is the mass of stars per Lyman continuum photon = 3.4 10^{-47} $M_\odot$/photon sec^{-1}.*)
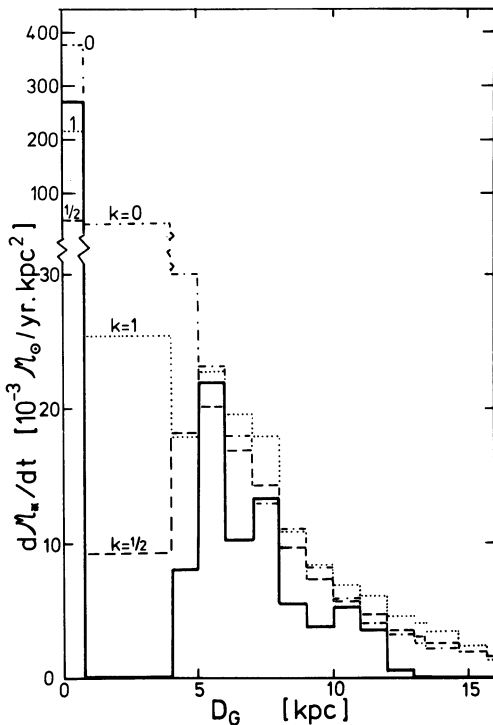

Figure 12: Observed star formation rates averaged over annuli in the galactic plane, compared to predicted rates for various values of k. The values on the ordinate are correct for k=1/2; for k=0,1,2 they must be multiplied by 1.49, 0.74, 0.58, respectively.

---

*) This differs from the value from Mezger et al (1974 because of the different IMF, different mass limits (Mezger et al used 35 and 0.6 $M_\odot$) and because Mezger et al made an error of 1n10; that the numbers differ by only 30% is coincidence. As a result, SBM's derived star formation rates are not significantly different from MS's.

t(HII) is the lifetime of radio HII regions, estimated by SBM at $5 \cdot 10^5$ years. 1.175 is the correction factor for non-giant HII regions in inter-arm regions. The entire factor equals $8 \cdot 10^{-53}$ $M_\odot$ year^{-1} /photon sec^{-1} absorbed in giant HII regions. For a given value of k, the possible error is (+100%, -25%) in $\langle M \rangle / \langle N_C \rangle$ due to uncertainty in the mass limits; the difference between various k's is $\sim$50%. Uncertainty in t(HII) is a factor of 2 and thus the uncertainty in the conversion factor is large. However, the *shape* of the star formation rate as a function of distance from the center depends only on the accuracy of the photon counting (which is high) and the assumption that the conversion factor is constant throughout the Galaxy. The latter is probably a reasonable assumption in all spiral arm regions, but is *ad hoc* for the galactic center.

The predicted star formation rates for various values of k were derived from numerical models of the type described by Biermann (1976). Stars are evolved according to tracks in the modern literature and, at the end of the red giant phase, stars between 0.7 and 6.7 $M_\odot$ return all but 0.7 $M_\odot$ to the IS medium and stars > 6.7 $M_\odot$ return all but 1.4 $M_\odot$. The fraction of material so returned, averaged over the IMF, is the 'return fraction', r. The returned material has heavy element abundances as calculated by Talbot and Arnett (1974) and zero deuterium.

k	Z	Z_D
2	0.16	10^{-9}
1	0.10	$1.3 \cdot 10^{-6}$
1/2	0.06	$1.5 \cdot 10^{-5}$
obs.	0.02	$2.0 \cdot 10^{-5}$

Table 1
Properties of Models

For D_G > 5 Kpc, the relationship between observed and predicted rates does not depend significantly on k. Only for D_G < 5 Kpc, where the remaining gas fraction is very small, does k become critical. Of the models calculated, k=1/2 gives the best fit, showing a minimum in the 1-4 Kpc range, as observed.

SBM also predict other parameters of the Galaxy, of which the D and heavy element abundances are extremely sensitive to k. Predicted values for the present time in the solar neighbourhood are given in Table 1 for k=1/2, 1 and 2. The sensitivity of Z and Z_D to k is due to the corresponding change in the IMF, which, for k > 0 has many more massive stars. Thus, k=1 or 2 produce far too many metals, by factors of 8 & 5 respectively. k=1/2 is best, producing only a factor 3 too many metals. This is probably within the accuracy of Talbot and Arnett's enrichment calculations.

Deuterium is destroyed by astration: the fraction of material astrated during the life of the Galaxy depends on k. We adopt an initial value of the D abundance equal to 10^{-4} by mass, near to the maximum allowed by

Wagoner's (1971) models and the observed present density of galaxies in the universe (ρ_G = 2 10^{-31}g cm^{-3}). The observed present value (Rogerson and York, 1973) is (1.4±0.2) 10^{-5} by number. Of the models calculated, k=2 predicts destruction of essentially all primordial D, k=1 leaves a value 15 times less than observed, k=1/2 leaves a value only a factor 1.3 less than observed.

k=1/2 would appear to be the solution providing fewest problems, from the point of view of: aesthetics, i.e. a monotonic IMF (see Schmidt 1963 and Fig. 11); agreement with the cluster IMF (see Fig. 11); prediction of $dM_\star/dt$ as a function of D_G; and prediction of local metal and D abundances. Audouze et al (1975) get reasonable agreement for isotope ratios with k=1 and r=0.5. If an IMF extending to 0.01 $M_\odot$ were adopted in the present experiment, the derived k would increase to $\sim$1.

k=1/2 to 1 is a lower dependence of the gas mass than is generally favoured. We emphasize that, in this experiment, the mass of gas is a parameter for time, metal abundance, etc. Our conclusion is that $dM_\star/dt$, as a function of time, in our Galaxy, is best represented as a dependence on $(M_{gas})^{1/2}$.

3) As a Function of Distance from the Galactic Center

The SBM analysis considers evolution of each annulus of the Galaxy, assumed isolated from all others, as a function of time. The rate constant, τ, for each annulus, is set to obtain the present day ratio of gas to stellar mass. We plot, in Fig. 13, Q, the inverse of the proportionality constant between $dM_\star/dt$ and $(M_{gas})^k$ i.e.

$$dM_\star/dt = Q^{-1}(M_{gas})^k \qquad (3)$$

$$\text{where} \quad Q = \tau\,(1-r)\,(M_{tot})^{k-1}$$

No matter what k one adopts, Q increases with distance from the center. This presumably corresponds, physically, to decreasing strength of the shock waves on the inner edges of the spiral arms.

Fig. 13 also shows Z and y predicted from the model with k=1/2, and observed y^+ and T_e for galactic HII regions. The predicted Z is normalized to 0.02 in the solar neighbourhood. y assumes a primodial value of 7% and is normalised to 10% in the solar neighbourhood, i.e. y=7+1.5Z where y is a number fraction and Z is a mass fraction, according to common usage. The observed points, both y^+ and T_e, are from Churchwell et al (in preparation). The decrease in T_e from 10 to 5 Kpc (first noted by Churchwell and Walmsley, 1975 and confirmed by Viner et al, 1976) can only be explained by an increase in Z by a factor 2. This would logically be associated with a corresponding increase in the dust/gas ratio. If the dust is selectively absorbing (as asserted by Mezger et al, 1974; Mezger & Smith, 1976) it will account for the change in y^+ over this radius interval. T_e does *not*, however, decrease further from 5 to 0 Kpc, indica-
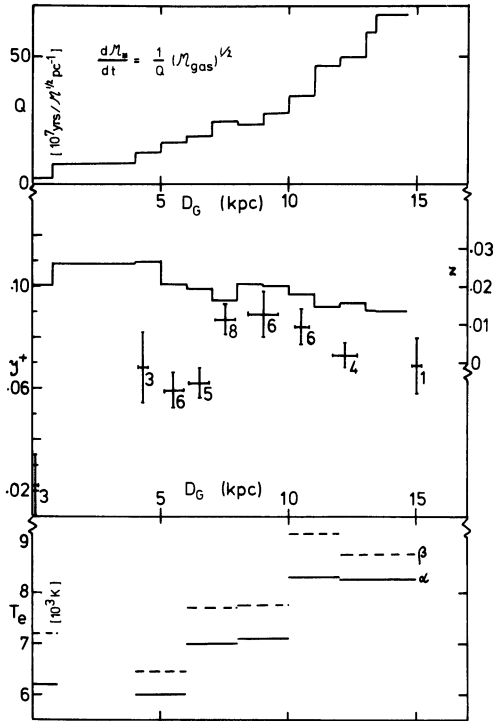
Figure 13: Observed and pre-
dicted (k=1/2) properties of
the Galaxy as a function of
distance from the center: a)
the inverse of the proportiona-
lity constant; b) predicted Z
and y compared to observed y^+
vertical error bars are mean
errors, the number of HII re-
gions in each interval is indi-
cated; c) median electron tem-
peratures of HII regions de-
rived from α and β line to con-
tinuum ratios. Observed data
is from Churchwell et al (in
preparation).

ting no further rise in Z, which is in agreement with the model predic-
tions. The reason for the flat Z distribution and high star formation
rate at low D_G is the return of material from large numbers of low mass
stars.

Returning to the star formation rates: The agreement between ob-
served and predicted rates in the main spiral arm region, between 5 and
12 Kpc is good. Outside 12 Kpc, the observed rate is about three orders
of magnitude too low. There are several possible explanations, of which
the most likely is that radial flow has reduced M_{gas}/M_{tot} from the value,
~ 1, corresponding to the low star formation rate observed. An alternative
explanation is that the star formation rate has been underestimated. How-
ever, the observed 7% He^+ abundance in the outer region supports a low
star formation rate. The low He^+ abundance is derived from 5 HII regions
at $D_G > 12$ Kpc; it cannot be explained by ionization effects. The value
agrees with that derived by d'Odorico et al (1976) based on two planetary
nebulae at $D_G > 12$ Kpc, and probably represents the primordial He abun-
dance, there having been essentially no star formation and no enrichment
in these regions.

The region between 0.8 and 4 Kpc is more complex. M_{gas} is low and
M_{gas}/M_{tot} even lower. For a high return rate, it is difficult to achieve
a very low gas fraction in a closed volume. It is probable that the O
star formation rate is less than expected because there are no shock
waves to trigger their formation. The gas fraction is probably kept small
by a high formation rate of low mass stars and/or mass flow into the ga-
lactic center.

In the center itself, $k=1/2$ predictes $53 \cdot 10^{-10}$ $M_\odot$ yr^{-1} pc^{-2} compared to $270 \cdot 10^{-10}$ observed. The predicted rate in this region is enormously sensitive to k. It will also be increased if there is gas flow from the surrounding area. Thus, it appears plausible that the very high rate in the galactic center can be maintained by returned mass from stars and in-flow from the immediate surrounding region of the disk. It is also pos-sible that the star formation rate is not constant and/or that the IMF in this region has more massive stars.

We want to thank all our colleagues from the MPIfR and from abroad whose communication of not yet published results and whose critical re-marks helped us to prepare this review paper.

REFERENCES

Audouze, J., Lequeux, J., Vigroux, L. 1975, Astron. Astrophys. 43, 71.
Beetz, M., Elsässer, H., Weinberger, R. 1974, Astron. Astrophys. 34, 335.
Beetz, M., Elsässer, H., Poulakos, C., Weinberger, R. 1976, Astron. Astro-
    phys. 50, 41.
Biermann, P. 1976, Astron. Astrophys. (in press).
Blaauw, A., 1964, Ann. Rev. Astron. Astrophys. 2, 213.
Blair, G.N., Peters, W.L., Vanden Bout, P. 1975, Astrophys. J. 200, L161.
Brown, R.L., Gammon, R.H., Knapp, G.R., Balick, B. 1974, Astrophys. J.
    192, 607.
Brown, R.L., Zuckerman, B. 1975, Astrophys. J. 202, L125.
Chaisson, E.J., Willson, R.F. 1975 Astrophys. J. 199, 647.
Churchwell, E., Walmsley, C.M. 1975, Astron. Astrophys. 38, 451.
Davidson, K., Harwit, M. 1967, Astrophys. J. 148, 443.
Davies, R.D. 1974, IAU Symposium No. 60, ed. F.J. Kerr and S.C. Simonson
    (Reidel, Dordrecht), p. 275.
Dickman, R.L. 1975a, Unpublished thesis, Columbia University.
Dickman, R.L. 1975b, Astrophys. J. 202, 50.
Downes, D. 1974, Proc. of the ESLAB Symposium HII Regions and the Galactic
    Center, ESRO-SP105, ed. A.F.M. Moorwood, p.247.
Elmegreem, B.G., Lada, Ch.J. 1976, (preprint).
Emerson, J.P., Furniss, I., Jennings, R.E. 1975, Mon. Not. R. Astr. Soc.
    172, 411.
Emerson, D.T. 1974, Mon. Not. R. Astr. Soc. 169, 607.
Encrenaz, P.J., Falgarone, E., Lucas, R. 1975, Astron. Astrophys. 44, 73.
Fazio, G.G., Wright, E.L., Zeilik II, M., Low, F.J. 1976, Astrophys. J.
    206, L165.
Gatley, I., Becklin, E.E., Mathews, K., Neugebauer, G., Penston, M.V.,
    Scoville, N. 1974, Astrophys. J. 191, L121.
Georgelin, Y.M., Georgelin, Y.P. 1976, Astron. Astrophys. 49, 57.
Gordon, M.A., Burton, W.B. 1976, Astrophys. J. 208, 346.
Grasdalen, G.L., Strom, K.M., Strom, S.E. 1973, Astrophys. J. 184, L53.
Grasdalen, G.L. 1976, Astrophys. J. 205, L83.
Habing, H.J., Goss, W.M., Matthews, H.E., Winnberg, A. 1974, Astron.
    Astrophys. 35, 1.
Harris, S., Wynn-Williams, C.G. 1976 Mon. Not. R. Astr. Soc. 174, 649.
Harris, S., Scott, P.F. 1976, Mon. Not. R. Astr. Soc. 175, 371.

Harten, R. H. 1976, Astron. Astrophys. 46, 109
Harvey, P. M., Gatley, I., Werner, M. W., Elias, J. H., Evans II, N. J.,
    Zuckerman, B., Morris, G., Sato, T., Litvak, M. M. 1974, Astrophys. J.
    189, L87
Herbig, G. H. 1960, Astrophys. J. Suppl. 4, 337
Herbig, G. H. 1962, Adv. Astron. Astrophys. 7, 47
Herbig, G. H. 1970, Proc. of the XVIth Liège Symp. 59, 13
Herbst, E., Klemperer, W. 1976, Phys. Today 29, 32
Hudson, H. S., Soifer, B. T. 1976, Astrophys. J. 206, 100
Hughes, V. A., Viner, M. R. 1976, Astrophys. J. 204, 55
Iben, I., Talbot, R. J. 1966, Astrophys. J. 144, 968
Israel, F. P., Habing, H. J., de Jong, T. 1973, Astron. Astrophys. 27, 143
Israel, F. P. 1976, Astron. Astrophys. 48, 193
Kahn, F. D. 1974, Astron. Astrophys. 37, 149
Knapp, G. R., Brown, R. L., Kuiper, T. B. H. 1975, Astrophys. J. 196, 167
Krügel, E., Mezger, P. G. 1975, Astron. Astrophys. 42, 441
Kutner, M. L., Evans II, N. J., Tucker, K. D. 1976 (preprint)
Lada, C. J., Gull, T. R., Gottlieb, C. A., Gottlieb, E. W. 1976a,
    Astrophys. J. 203, 159
Lada, C. J., Dickinson, D. F., Gottlieb, C. A., Wright, E. L. 1976b,
    Astrophys. J. 207, 113
Lada, Ch. J. 1976, Astrophys. J. Suppl. Series (in press)
Larson, R. B. 1969a, Mon. Not. R. Astr. Soc. 145, 271; 1969b, ibid 145, 297
Larson, R. B., Starrfield, S. 1971, Astron. Astrophys. 13, 190
Lect. Notes in Phys. 42, 1975, Proc. of the Symposium HII regions and re-
    lated topics, eds. T. L. Wilson and D. Downes (Springer Verlag,
    Heidelberg)
Liszt, H. S. 1973, Unpubl. thesis, Princeton Univ.
Lo, K. Y. 1974, Unpubl. thesis, Mass. Inst. Technology.
Lo, K. Y., Burke, B. F., Haschick, A. D. 1975a, Astrophys. J. 202, 81
Lo, K. Y., Walker, R. C., Burke, B. F., Moran, J. M., Johnston, K. J.,
    Ewing, M. S. 1975b, Astrophys. J. 202, 650
Loren, R. B., Vanden Bout, P. A., Davis, H. J. 1973, Astrophys. J. 185, L67
Loren, R. B. 1975, Nat. Sci. Foundation Technical Rep. MPS-05070-75-1
Mader, G. L., Johnston, K. J., Moran, J. M., Knowles, S. H., Mango, S. A.,
    Schwartz, P. R., Waltman, W. 1975, Astrophys. J. 200, L111
Madore, B. F., Van den Bergh, S., Rogstad, D. H. 1974, Astrophys. J. 191, 317
Mathews, W. 1969, Astrophys. J. 157, 583
Mathewson, D. S., Kruit, P. C. van der, Brouw, W. N. 1972, Astron. Astro-
    phys. 17, 468
Mezger, P. G. 1971, Highlights of Astronomy 2, ed. C. de Jager
    (Reidel, Dordrecht) p. 367
Mezger, P. G., Smith, L. F., Churchwell, E. 1974, Astron. Astrophys. 32, 269
Mezger, P. G., Wink, J. 1974, Mem. Soc. Astr. Italiana, 45, 315
Mezger, P. G. 1974, Proc. ESO/SRC/CERN Conference of Research Programmes
    for the New Large Telescopes, ed. A. Reiz, p. 79
Mezger, P. G. 1975, Structure and Evolution of Galaxies, ed. G. Setti,
    (Reidel, Dordrecht) p. 174
Mezger, P. G., Smith, L. F. 1975, Stars and Galaxies from Observational
    points of view, ed. E. K. Kharadze, (Acad. Sci. Georgian SSR) p. 369
Mezger, P. G., Wink, J. 1976, Astrophys. Space Sci. Library (Reidel,
    Dordrecht) in press

Mezger, P. G., Smith, L. F. 1976, Astron.Astrophys. 47, 143

Milman, A. S. 1975, Unpubl. thesis, Univ. of Maryland

Milman, A. S., Knapp, G. R., Kerr, F. J., Knapp, S. L., Wilson, W. J. 1975, Astrophys. J. 80, 93

d'Odorico, S., Peimbert, M., Sebbadin, F. 1976, Astron. Astrophys. 47, 341

Pankonin, V., Walmsley, C. M. 1976, Astron. Astrophys. 48, 341

Penzias, A. 1975, Atomic and Molecular Physics and the Interstellar Matter, ed. Roger Balian, (North-Holland, Amsterdam),p. 375

Roberts, M. S. 1957, Publ. Astr. Soc. Pacific 69, 59

Rogerson, J. B., York, D. G. 1973, Astrophys. J. 186, L95

Salpeter, E. E. 1955, Astrophys. J. 121, 161

Schmidt, M. 1959, Astrophys. J. 129, 243

Schmidt, M. 1963, Astrophys. J. 137, 758

Scoville, N. Z., Solomon, P. M., Penzias, A. A. 1975, Astrophys. J. 201, 352

Simon, M., Righini, G., Joyce, R. R., Gezari, D. Y 1973, Astrophys. J. 186, L127

Snyder, L. E., Buhl, D. 1975, Astrophys. J. 197, 329

Strel'nitskii 1975, Sov. Phys. - Usp. 17, 507

Sullivan III, W. T., Downes, D. 1973, Astron. Astrophys. 29, 369

Talbot, R. J. Jr., Arnett, W. D. 1974, Astrophys. J. 190, 605

Van den Bergh, S. 1961, Astrophys. J. 134, 554

Viner, M. R., Clarke, J. N., Hughes, V. A. 1976, Astrophys. J.(in press)

Vrba, F. J., Strom, K. M., Strom, S. E., Grasdalen, G. L. 1975, Astrophys. J. 197, 77

Wagoner, R. V. 1971, Highlights of Astronomy 2, ed. C. de Jager, (Reidel, Dordrecht), p. 301

Williams, I. P., Cremin, A. W. 1969, Mon. Not. R. Astr. Soc. 144, 359

Woodward, P. R. 1976, Astrophys. J. 207, 484

Wynn-Williams, C. G., Becklin, E. E., Neugebauer, G. 1972, Mon. Not. R. Astr. Soc. 160, 1

Wynn-Williams, C. G., Becklin, E. E. 1974, Publ. Astr. Soc. Pacific 86, 5

Yorke, H. W., Krügel, E. 1976, Astron. Astrophys. (in press)